Analyst

COMMUNICATION

View Article Online
View Journal

Cite this: DOI: 10.1039/c5an00737b

Received 16th April 2015,
Accepted 15th May 2015

DOI: 10.1039/c5an00737b

www.rsc.org/analyst

FT-IR imaging for quantitative determination of liver fat content in non-alcoholic fatty liver†

K. Kochan,[a,b] E. Maslak,[a] S. Chlopicki[a,c] and M. Baranska*[a,b]

In this work we apply FT-IR imaging of large areas of liver tissue cross-section samples (~5 cm × 5 cm) for quantitative assessment of steatosis in murine model of Non-Alcoholic Fatty Liver (NAFLD). We quantified the area of liver tissue occupied by lipid droplets (LDs) by FT-IR imaging and Oil Red O (ORO) staining for comparison. Two alternative FT-IR based approaches are presented. The first, straightforward method, was based on average spectra from tissues and provided values of the fat content by using a PLS regression model and the reference method. The second one – the chemometric-based method – enabled us to determine the values of the fat content, independently of the reference method by means of *k-means* cluster (KMC) analysis. In summary, FT-IR images of large size liver sections may prove to be useful for quantifying liver steatosis without the need of tissue staining.

Introduction

Non-alcoholic fatty liver disease (NAFLD) is a chronic liver disorder, primarily manifested by an increased accumulation of lipids within the tissue, in the form of lipid droplets (LDs).[1] In the early stage of NAFLD it is difficult to diagnose this disease due to the lack of both: clear and specific symptoms as well as diagnostic methods. The early stage of NAFLD (fatty liver) may progress to non-alcoholic steatohepatitis (NASH) and cirrhosis,[2] which finally leads to irreversible liver damage and failure. It is not until the advanced stage of liver damage, affecting the functioning of the whole body, that the symptoms of NAFLD (although still non-specific) become clearly visible. Obviously, diagnosis of the disease at an advanced stage significantly reduces the chances of successful therapy.

The importance of NAFLD relates not only to the fact that it is widespread (WHO estimates that fatty liver affects approximately 30% of the human population of the world)[3] but more importantly, because it represents a manifestation of a metabolic syndrome[4] that is associated with diabetes mellitus type II and impose the increased risk of cardiovascular diseases.[5] In fact, the association of hepatic steatosis with diabetes and cardiovascular diseases is well established and was reported numerous times.[6,7] The nature of this relationship however, just like the very emergence and development of fatty liver, still remains unclear. NAFLD, often preceding the development of mentioned diseases, is increasingly seen as their common initial state, which can evolve in each of these.[8]

The lack of a good diagnostic method creates a need in this field, which is not easy to accomplish, since an approach to diagnose early NAFLD would need to be sensitive to small changes of biochemical contents of the liver.

Fourier transform infrared (FT-IR) spectroscopy is a method that possesses huge potential in the field of diagnostics.[9–13] Primarily, it does not require any special sample preparation. Moreover, this technique is adaptable to different types of preparation procedures, including formalin fixed and paraffin embedded specimens, which are known to preserve the structural composition in a good way.[10] Secondly, FT-IR is a sensitive method to obtain information about the biochemical composition of the sample without the use of stains (in the case of which the number of dyes possible to be used on the same sample is limited). Moreover, FT-IR is a relatively quick technique of spectroscopic imaging that allows examination of representative areas of samples. The use of infrared radiation as a source of excitation minimalizes the possibility of a destructive impact of the measurement on the sample.

Infrared imaging has been successfully applied for studies of different tissues and cells including liver,[10,11] brain,[12,13] lungs,[14] cervix,[15] and aorta.[16] As for liver this technique was mostly used to examine cancer.[10,11] IR spectroscopy however is perfectly suited to analyse tissue contents of lipids, as has been repeatedly proven in various tissues.[17–20] Both signals in the high wavenumber range (2800–3100 cm^{-1}) as well as

[a]Jagiellonian Centre for Experimental Therapeutics (JCET), Jagiellonian University, Krakow, Poland. E-mail: baranska@chemia.uj.edu.pl
[b]Faculty of Chemistry, Jagiellonian University, Krakow, Poland
[c]Department of Experimental Pharmacology, Jagiellonian University Medical College, Krakow, Poland

†Electronic supplementary information (ESI) available. See DOI: 10.1039/c5an00737b

within the fingerprint region (*i.e.* the band at approximately 1740 cm^{-1}) are well suitable for demonstrating the presence of lipids. In addition, IR spectra allowed for a detailed investigation of the nature of lipid compounds of the sample, providing for example information on the presence of unsaturated bonds or cholesterol and its esters.[15] The quantitative approach to tissue analysis with the use of FT-IR imaging is, however, not common. Only a few examples can be found in the literature.[20] In addition, quantitative determination *via* FT-IR requires supporting results, obtained from the other method, as absolute quantification through spectral data itself is not possible.[21]

The aim of this work was to develop a methodology for infrared imaging-based quantitative analysis of liver steatosis using a murine model of NAFLD and therefore elaborate new tools applicable for fixed tissue sections.

In the present work we used a dietary mouse model of non-alcoholic fatty liver. Fatty liver was induced in C57BL/6J male mice by feeding for 15 weeks with a high fat diet (HFD), containing 60 kcal% fat (Harlan Laboratories, Germany). For the last 5 weeks of HFD feeding, some mice were subjected to anti-steatotic treatment, so the liver taken from a group of 13 animals had varying degrees of steatosis. After 15 weeks of HFD feeding the mice were euthanized by injection of ketamine (100 mg kg^{-1}) with xylazine (10 mg kg^{-1}). The livers were collected immediately after euthanizing the animals and were frozen in optimum cutting temperature (OCT) medium at −80 °C. Direct preparation of tissue for measurement included cutting it into slices of 10 μm thickness in a cryostat chamber (Leica CM 1950) at −23 °C. Tissue sections were subsequently placed on CaF_2 slides and fixed with 4% buffered formalin solution for 10 minutes. The remainders of the fixative were washed out with distilled water (2 × 5 min).

FT-IR measurements on a macro scale were performed with the use of a spectrometer FT-IR Varian 670 equipped with a microscope (15× cassegrain objective) and a 128 × 128 MCT Focal Plane Array detector. All spectra were recorded with a spectral resolution of 8 cm^{-1} in the spectral range from 900 to 3800 cm^{-1} in the transmission mode, by accumulating 64 scans. The imaged areas were approximately ~5 × 5 cm.

Data analysis was performed with the use of Varian Resolution Pro Software, as well as Cytospec and MatLab. The integration of the band areas was performed in Opus Software. Data preprocessing included: baseline offset correction, normalisation to the amide I band (1620–1680 cm^{-1}) and a quality test (to remove pixels representing the background as well as distorted) performed on the basis of sample thickness criterion in the range 1620–1680 cm^{-1}. *K-means* cluster analysis was performed in the range 1420–1760 cm^{-1} with the use of 2nd derivatives (calculated with Savitzky–Golay algorithm and 9 smoothing points). The number of classes differed between samples, but typically not exceeding 4.

As a reference method histochemical staining with Oil Red O was used. Oil Red O is a standard diazo dye for lipids and triglycerides. The procedure of staining involved application of solutions for a certain amount of time, according to the following steps: deionized water (3 min), 60% isopropanol alcohol (2 min), Oil Red O (30 min) and deionized water (1 min). Afterwards the slides with tissues were covered with glycerol gel. The % of tissue covered by lipid droplets was calculated with the Columbus Image Data Storage and Analysis System (PerkinElmer, USA) adapted for the Oil Red O stained sections algorithm.

Results and discussion

ORO staining

The first approach to analyse the obtained data was a general assessment of the fat content within the liver tissue with the use of a "gold standard" method – histochemical staining with Oil Red O (ORO). Fig. 1 presents the results of ORO staining on the basis of which the assessment of the level of steatosis was made: representative stained sections with various contents of the fat (Fig. 1A) and obtained results, expressed as a percentage of the tissue surface occupied by the lipid droplets (Fig. 1B).

As can be seen, the degree of fat content was quite different within the studied group (~2–42%), as intended, and thus provided an appropriate series of samples to validate the use of FT-IR for the liver fat content analysis. The ORO staining results reflect well the content of fat within the tissue. On the one hand, they allow for a rapid assessment of the overall con-

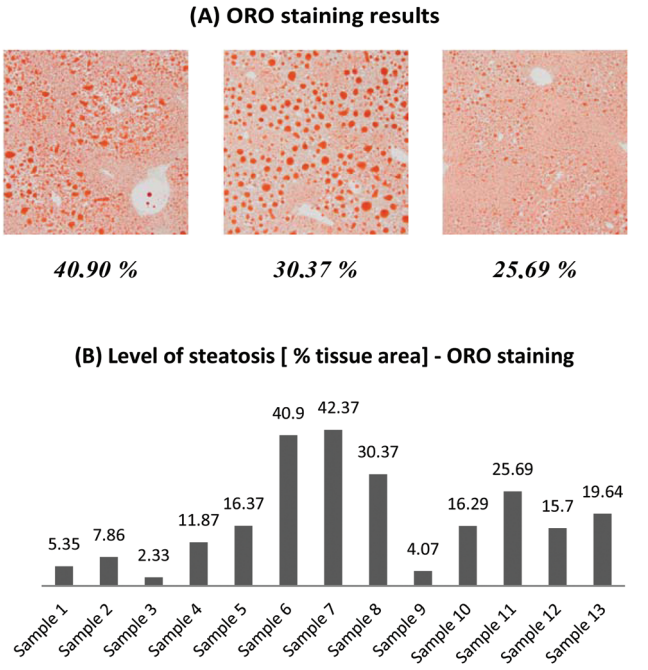

Fig. 1 (A) ORO stained sections (magnification 100×) from 3 representative samples with different levels of steatosis (with the percentage of fat specified under the photograph) along with (B) the level of steatosis expressed as a % of tissue area occupied by lipid droplets. The percentage values (given above each bar and below each photograph) were calculated by Columbus Software.

ditions of the organ, while on the other hand they enable a more detailed, quantitative research.

FTIR based approaches

The presented approaches involved FT-IR imaging of the whole liver tissue cross-sections. The condition for the correctness of their application is imaging of the whole tissue sections. Even though a healthy liver is homogeneous, the pathologically changed liver was featured by heterogeneity and unevenly distributed lipid droplets in different parts of the liver tissue.

Approach 1: a PLS model based on average spectra for each tissue section

The first FT-IR approach is based on obtaining average spectra for each tissue section. After extraction of such spectra, the removal of the baseline and the normalization to the amide I band, two ratios of intensities were calculated: of the high wavenumber range (2800–3100 cm^{-1}) to the amide I band and of the area of the band located at 1740 cm^{-1} (C═O stretching vibration[20]) to the amide I band. Ratios calculated in such a way, preceded by normalization of all spectra to the amide I band, represent the content of lipids within each tissue in a straightforward manner. Fig. 2 presents the calculated ratios from FT-IR averaged spectra of whole tissues.

By comparing the IR-based results from Fig. 2A and B with the ORO assessment, it can be seen that the trend of changes between samples is well preserved by both chosen ratios. However, the ORO-based approach presents the results in a way that magnifies the differences between the content of lipids in different tissue sections. In the IR-based approach the differences between the extreme samples do not appear to be so big (compare the relationship between samples 3 and 6 in Fig. 1B, 2A and B). The reason for that is, however, very simple. The appearance of lipid droplets in healthy liver is not excluded entirely, as they can occur in healthy tissues as well, but they are not present in high amounts. Therefore, the percentage of the tissue area occupied by LDs can vary practically from none or very low to very high. Due to this, in the case of the ORO assessment, the scale of the results varies between 0 and 100. The IR-based approach, on the other hand, involves the use of spectra averaged across the tissue. In such a spectrum both chosen signals, the band at 1740 cm^{-1} and the bands in the range 2800–3050 cm^{-1} will never be completely absent.

In order to improve the chosen criterion, both ratios (1740 cm^{-1}/amide I and 2800–3050 cm^{-1}/amide I) were calculated for healthy liver tissue sections, with the use of identical pre-treatment of spectra. The results obtained for the whole sample set were decreased by the values obtained for samples of healthy liver (1740/amide I: 0.07 and 2800–3050/amide I: 0.46). The corrected FT-IR band ratios (Fig. 2C and D) reproduced the ORO results better and can be used to estimate the level of steatosis.

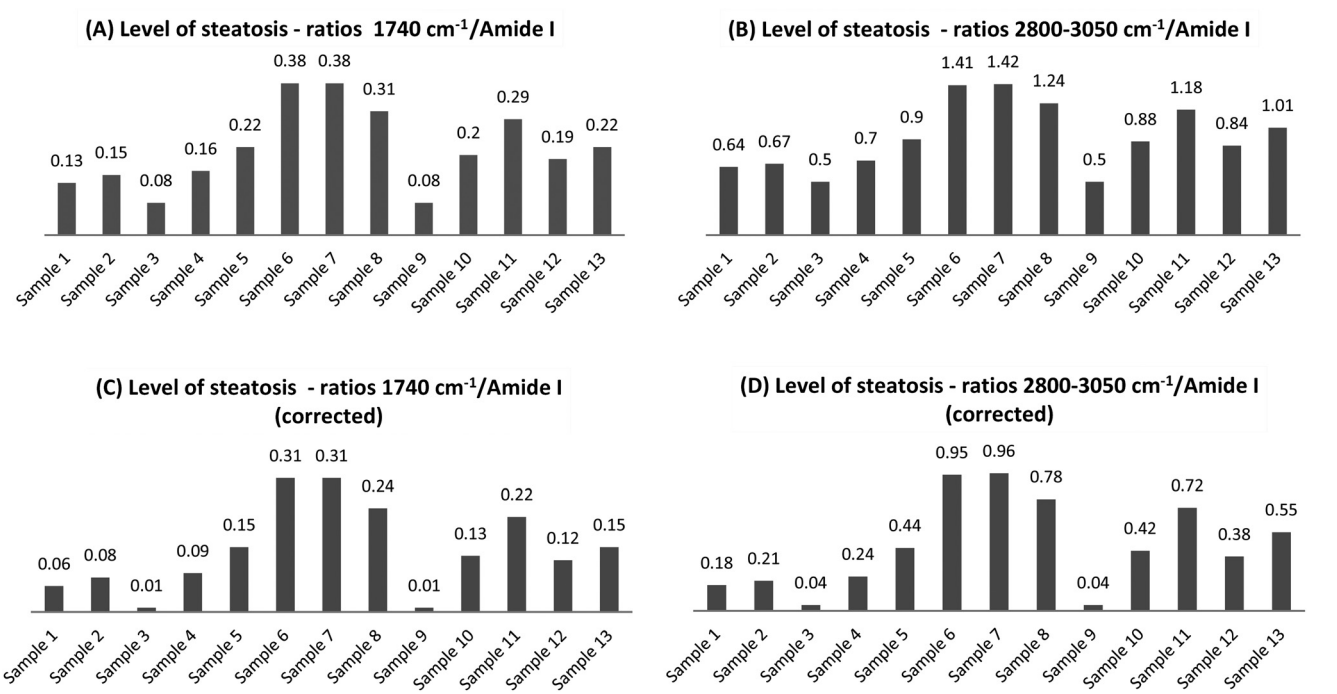

Fig. 2 The values calculated from FT-IR spectra (obtained by averaging the whole tissue measurement), presenting the ratios of chosen bands: (A) at 1740 cm^{-1} to the amide I band (1620–1680 cm^{-1}) and (B) the high wavenumber range (2800–3050 cm^{-1}) to the amide I band (1620–1680 cm^{-1}). Panels (C) and (D) represent the same data set, but the values are decreased by the value obtained for the control samples (livers from healthy mice). The presented values were calculated for spectra normalised to the amide I band to reflect more strictly the differences between the levels of lipids within the tissue.

Table 1 Parameters of the PLS regression model

Parameter	Value	Parameter	Value
Slope	0.9805945	R-square	0.9805948
Offset	0.363441	RMSEC	2.0094995
Correlation	0.9902497	SEC	2.1482458
R^2 (Pearson)	0.9805945	Bias	-4.7684×10^{-7}

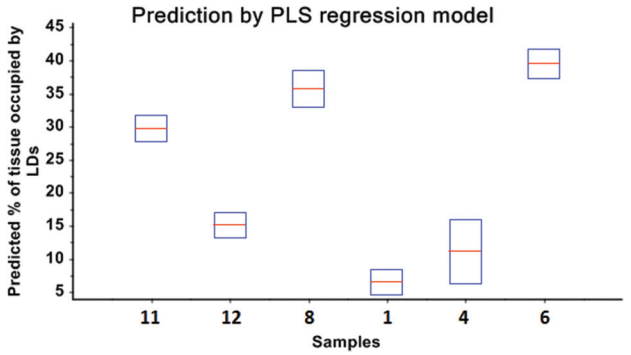

Fig. 3 Results of prediction of the percentage of tissue occupied by LDs performed with the use of a built PLS model for the validation set (value – red line, standard deviation – blue squares). The PLS model is based on FT-IR spectra averaged for whole tissue sections, in the range 1580–1780 cm^{-1}.

For the FT-IR averaged spectra of tissues a PLS regression model for the prediction of the level of steatosis (percentage of the tissue area occupied by LDs) was built. The data set was divided into two: calibration and validation sets. Each of them contained samples differing in the level of steatosis. Different pre-treatment procedures and spectral ranges were tested, but eventually the best results were obtained for the model where the pre-treatment of spectra remained the same as for the calculation of ratios and the spectral range of 1580–1780 cm^{-1} was included. The parameters of the PLS model (on the basis of the calibration set) are presented in Table 1. The results of prediction performed with the use of it on the validation model are presented in Fig. 3 (and Table S1, ESI†).

The model allowed for a successful prediction of the percentage of tissue covered by lipid droplets, although the standard deviation appears to be higher for tissues with medium developed steatosis. Nonetheless, the predicted values remain in good agreement with the ORO-based results (see Table 2, summarising the FT-IR based approaches).

Approach 2: the ratio of pixels assigned to the lipid class to all pixels

The second possible FT-IR approach involves the use of entire spectral images, obtained for large areas of tissue sections. By performing cluster analysis (*k-means*) on the FT-IR images obtained, it is possible to separate a class of clearly higher lipid contents. Subsequently, analogously to the ORO-based approach, by calculating the ratio of pixels assigned to the lipid class to all pixels representing the tissue it is possible to determine the percentage of tissue occupied by LDs. An example of this approach is presented in Fig. 4.

Table 2 Results of the assessment of % of tissue occupied by LDs obtained with all presented approaches: from ORO staining and from FT-IR spectra: PLS-based and KMC-based analyses. The SD values for the PLS-based approach are presented in Table S1 (ESI)

	% of tissue occupied by LDs		
Sample	PLS	KMC	ORO
Sample 1	6.49	6.33	5.35
Sample 2	11.45	8.52	7.86
Sample 3	1.04	1.97	2.33
Sample 4	11.09	10.24	11.87
Sample 5	18.67	18.96	16.37
Sample 6	39.47	38.05	40.9
Sample 7	41.05	43.38	42.37
Sample 8	35.70	32.8	30.37
Sample 9	1.04	3.66	4.07
Sample 10	17.10	18.93	16.29
Sample 11	29.71	26.2	25.69
Sample 12	15.14	15.29	15.7
Sample 13	19.46	21.81	19.64

This approach, however, is associated with a certain error, especially in the case of microvesicular steatosis or any early stage of LD development. This results from the droplet size and shape. In cases of an early development or manifestation in the form of microvesicular steatosis, the droplet size tends to be below the spatial resolution of pixels in FT-IR images (~5 × 5 μm^2). Thus, the assessed value will be overestimated (when the droplet is smaller than the pixel but takes more than 50% of its area) or underestimated (if the droplet covers less than 50% of pixel area). This problem applies also to a more advanced stage, when single LD occupies an area of several pixels. Due to their round shape, droplets will never fit perfectly into the image constructed from square pixels. Moreover, the cluster analysis approach does not allow (in the case of attempts to develop a universal model) for a clear definition of when a class can be classified as a tissue and when as a LD. This is due to the fact that the lipid content (and therefore – spectrum) within the tissue (excluding lipid droplets) is different for the tissues with advanced steatosis and without it (or on early stage of development). In general, spectra of the "non-lipid" classes from livers with advanced steatosis present much more intense lipidic signals compared to "non-lipid" classes from healthy livers. Therefore, a clear criterion for the division between the lipid and non-lipid classes (*i.e.* a particular value of the lipid/protein ratio) that would be applicable for all tissues, regardless of the level of steatosis development cannot be defined. Each tissue should be rather considered individually.

Despite potential sources of errors described above, with a careful approach, it is possible to obtain the percentage values of tissue occupied by LDs. These results still remain in good correlation with the values obtained by the ORO-based

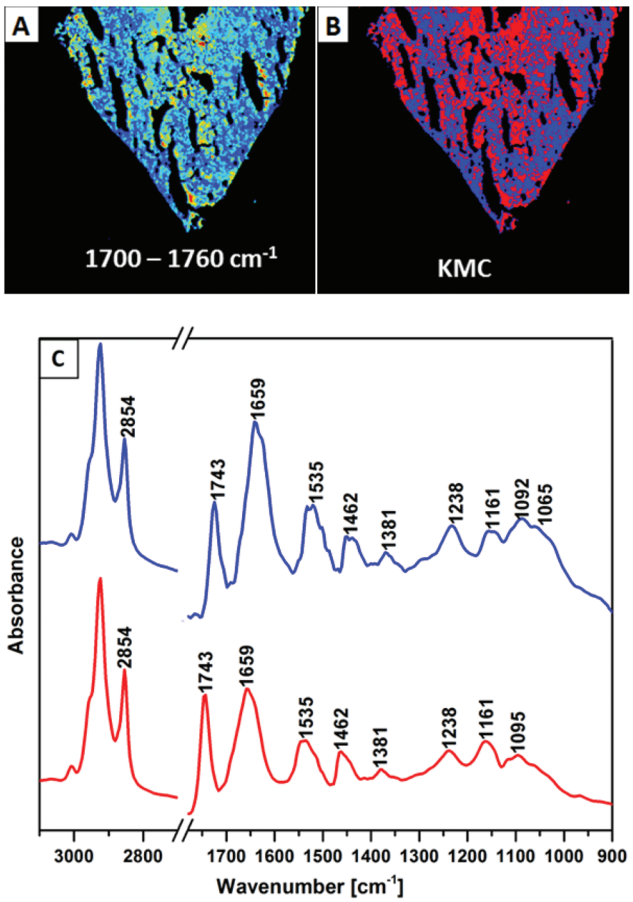

Fig. 4 An example of FT-IR results of large tissue section analysis: (A) integration of the C=O stretching band (in the range 1700–1760 cm^{-1}) along with the KMC results: (B) distribution of lipid classes (red) and (C) the corresponding KMC averaged spectra of classes assigned to most intense bands.

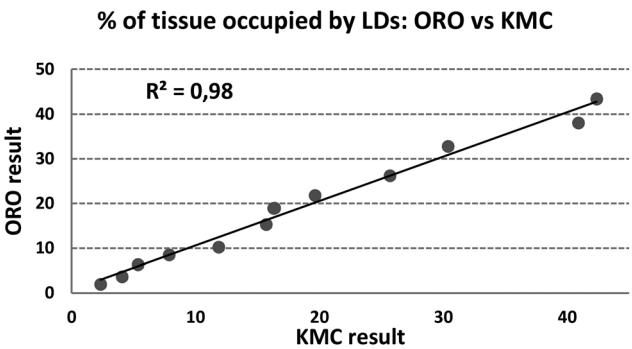

Fig. 5 Correlation between the percentage value of tissue occupied by LDs obtained by ORO-based and KMC-based approaches. Results from individual samples are given in Table 2.

approach (Fig. 5 and Table 2). Therefore, this approach – like the previous, based on average spectra – also appears to be suitable for assessment of the degree of steatosis development.

Conclusions

FT-IR imaging is a technique with huge potential in the field of the study of biological materials. The simplicity of sample preparation and the complexity of the obtained results make it a tool of choice for tissue studies. In addition, it provides a possibility not only to examine bigger groups of samples but also to investigate large areas, thereby eliminating both the impact of individual variability and randomness of the selection of the investigated area. In the present work we applied FT-IR imaging of large pieces of liver cross-sections for quantitative determination of the steatosis that was performed on the basis of percentage of liver tissue occupied by lipid droplets. We presented two approaches: the first, based on the averaged spectra of a tissue and the second, based on the KMC analysis of each imaged specimen. Both approaches enabled us to obtain results, which remain in a very good correlation with ORO results and therefore allowed us to achieve the same objective as ORO staining. In the case of spectroscopic methods, however, the obtained experimental data can be additionally analysed in terms of liver contents of other components. In the first approach presented in this work, a simple calculation of the ratio of lipid to protein bands (preceded by normalisation to the amide I band) provided in a straightforward manner to quantify the liver lipid content. By the use of a PLS regression model and results obtained with ORO staining, it was possible to obtain explicit values. The second approach proposed in this work allowed, in an analogous way to the ORO-based method, to assess the percentage of tissue affected by pathological steatotic changes. It is worth adding that the first approach did not require the use of any advanced chemometric methods and was easier to implement in terms of analysis. However, it did not allow us to determine the absolute value of the fat liver content without the aid of another technique. The second approach, in turn, required a more time-consuming analysis, but it enabled us to determine the absolute value of the fat content without the need of a reference method. Altogether, FT-IR imaging of large areas of liver cross-section seems to represent a powerful and reliable method for the quantitative assessment of liver steatosis that may prove to be useful to assess liver disease progression in animal models of NAFLD as well as in patients.

Acknowledgements

This work was supported by the European Union under the European Regional Development Fund (grant coordinated by JCET-UJ, POIG.01.01.02-00-069/09) and the National Science Center (grant DEC-2013/09/N/NZ7/00626).

Notes and references

1 R. Lomonaco, N. E. Sunny, F. Bril and K. Cusi, *Drugs*, 2013, 73(1), 1–14.

2 N. Bhala, P. Angulo, D. van der Poorten, E. Lee, J. M. Hui, G. Saracco, L. A. Adams, P. Charatcharoenwitthaya, J. H. Topping, E. Bugianesi, C. P. Day and J. George, *Hepatology*, 2011, **54**(4), 1208–1216.
3 World Health Organisation, WHO: http://www.who.int.
4 E. Vanni, E. Bugianesi, A. Kotronen, S. De Minicis, H. Yki-Järvinen and G. Svegliati-Baroni, *Dig. Liver Dis.*, 2010, **42**(5), 320–330.
5 P. L. Huang, *Dis. Models & Mech.*, 2009, **2**(5–6), 231–237.
6 K. H. Williams, N. A. Shackel, M. D. Gorrell, S. V. McLennan and S. M. Twigg, *Endocr. Rev.*, 2013, **34**(1), 84–129.
7 M. Gaggini, M. Morelli, E. Buzzigoli, R. A. DeFronzo, E. Bugianesi and A. Gastaldelli, *Nutrients*, 2013, **5**(5), 1544–1560.
8 Q. M. Anstee, G. Targher and C. P. Day, *Nat. Rev. Gastroenterol. Hepatol.*, 2013, **10**(6), 330–344.
9 K. Das, C. Kendall, M. Isabelle, C. Fowler, J. Christie-Brown and N. Stone, *J. Photochem. Photobiol., B*, 2008, **92**(3), 160–164.
10 K. Kochan, P. Heraud, M. Kiupele, V. Yuzbasiyan-Gurkan, D. McNaughton, M. Baranska and B. R. Wood, *Analyst*, 2015, **140**(7), 2402–2411.
11 K. Thumanu, S. Sangrajrang, T. Khuhaprema, A. Kalalak, W. Tanthanuch, S. Pongpiachan and P. Heraud, *J. Biophotonics.*, 2014, **7**(3–4), 222–231.
12 M. J. Hackett, J. Lee, F. El-Assaad, J. A. McQuillan, E. A. Carter, G. E. Grau, N. H. Hunt and P. A. Lay, *ACS Chem. Neurosci.*, 2012, **3**(12), 1017–1024.
13 N. Bergner, B. F. M. Romeike, R. Reichart, R. Kalff, C. Krafft and J. Popp, Clinical and Biomedical Spectroscopy and Imaging II, ed. N. Ramanujam and J. Popp, *Vol. 8087 of Proceedings of SPIE-OSA Biomedical Optics*, Optical Society of America, 2011, paper 80870X.
14 P. D. Lewis, K. E. Lewis, R. Ghosal, S. Bayliss, A. J. Lloyd, J. Wills, R. Godfrey, P. Kloer and L. A. J. Mur, *BMC Cancer*, 2010, **10**, 640.
15 B. R. Wood, L. Chiriboga, H. Yee, M. A. Quinn, D. McNaughton and M. Diem, *Gynecol Oncol.*, 2004, **93**(1), 59–68.
16 K. M. Marzec, T. P. Wrobel, A. Ryguła, E. Maślak, A. Jasztal, A. Fedorowicz, S. Chlopicki and M. Baranska, *J. Biophotonics.*, 2014, **7**(9), 744–756.
17 F. Kucuk Baloglu, S. Garip, S. Heise, G. Brockmann and F. Severcan, *Analyst*, 2015, **140**(7), 2205–2214.
18 M. J. Baker, J. Trevisan, P. Bassan, R. Bhargava, H. J. Butler, K. M. Dorling, P. R. Fielden, S. W. Fogarty, N. J. Fullwood, K. A. Heys, C. Hughes, P. Lasch, P. L. Martin-Hirsch, B. Obinaju, G. D. Sockalingum, J. Sulé-Suso, R. J. Strong, M. J. Walsh, B. R. Wood, P. Gardner and F. L. Martin, *Nat. Protocols*, 2014, **9**(8), 1771–1791.
19 S. G. Kazarian and K. L. A. Chan, *Biochim. Biophys. Acta,–Biomembr.*, 2006, **1758**(7), 858–867.
20 I. Dreissig, S. Machill, R. Salzer and C. Krafft, *Spectrochim. Acta, Part A*, 2009, **71**(5), 2069–2075.
21 K. M. Gough, D. Zelinski, R. Wiens, M. Rak and I. M. C. Dixon, *Anal. Biochem.*, 2003, **316**, 232–242.

